ECCOMAS Thematic Conference on Multibody Dynamics
July 24 - 28, 2023, Lisbon, Portugal

Local Isotropic Compliance in Planar Parallel 3RRR Manipulators

M. Verotti[1], **P. Masarati**[2], **M. Morandini**[2], **N. P. Belfiore**[3]

[1] Department of Mechanical, Energy, Management and Transport Engineering
University of Genoa
Via All'Opera Pia, 15, 16145 Genoa Italy
matteo.verotti@unige.it

[2] Dipartimento di Scienze e Tecnologie Aerospaziali
Politecnico di Milano
Via La Masa, 34, 20156 Milano Italy
[pierangelo.masarati, marco.morandini]@polimi.it

[3] Department of Industrial, Electronic and Mechanical Engineering
Roma Tre University
Via Vito Volterra, 62, 00146 Rome Italy
nicolapio.belfiore@uniroma3.it

ABSTRACT

In this paper, the local isotropic compliance property is investigated in the Special Euclidean Group SE(2). The relation between the generalized force applied to the end-effector and its consequent generalized displacement is evaluated considering the planar parallel 3RRR manipulator. A proper control action is defined in order to decouple the effects of forces and moments on the end-effector displacement and rotation, and to guarantee the condition of parallelism between force and displacement vectors. A numerical example is presented and the proposed approach is verified by performing several multi-body simulations.

Keywords: Isotropic compliance, Stiffness matrix, Active stiffness regulation, Screw theory

1 INTRODUCTION

Parallel manipulators received considerable attention in the last decades because of their considerable advantages with respect to their open-chain counterparts. Avoiding the pyramidal effect of serial robots, they guarantee high speed, rigidity, accuracy, stability, load capability and low inertia [1, 2, 3]. These manipulators have been implemented in many engineering fields, for industrial, space and medical applications [4]. Among parallel manipulators, planar ones have been considered for precision positioning applications, semiconductor manufacturing, automatic microassembly [5, 6]. In particular, the 3RRR manipulator assures three degrees of freedom with an architecture composed of three legs connecting the frame to the moving platform. Each leg is a serial chain with two passive revolute joints and an active one. Generally, the actuator is linked to the frame in order to reduce the inertia of the moving parts [7].

However, despite the numerous advantages, 3RRR manipulators present typical drawbacks of parallel robots: limited workspace and complex singularities. To reduce these disadvantages, many investigations focused on mathematical modeling aspects [8], synthesis procedures [9], kinematics performance [10] and singularity [11] analyses, path planning [12], or motion reliability [13].

Other investigations applied different control techniques to reduce these disadvantages or, more in general, to improve the performance of these manipulators. For example, proportional-derivative plus gravity compensation was implemented to compensate the positioning error caused by gravity force or dynamic disturbances [14, 15]. A real-time computed-torque control algorithm was

implemented to the Delta robot [16], whereas nonlinear adaptive control was considered in the Hexaglide for the minimization of the tracking error [17].

Focusing on the 3RRR, the extended computed torque control scheme, based on the use of extra sensors in the passive joints, was proposed to increase accuracy and precision [18]. A dynamic filtered path tracking control scheme was considered for reducing the positioning errors caused by backlash, system nonlinearities, and unknown disturbances [19]. In Ref [20], a visual servoing resolved acceleration control scheme was implemented to reduce the computational loads of the control loop and the tracking errors of the end-effector.

In recent investigations, a proportional controller has be implemented to achieve a particular kinetostatic condition in the Euclidean Group E(3), called isotropic compliance. Considering 3-DoF manipulators, isotropic compliance holds for a specific manipulator posture when the displacement of the end-effector is parallel to the external applied force [21]. This condition is achievable if the compliance matrix of the manipulator in the task space, regulated by means of the controller action, becomes a scalar matrix. The extension of the isotropic compliance property to the Special Euclidean Group SE(3), in case of 6-DoF [22] and redundant [23] serial manipulators, lead to the definition of two different cases: *local* isotropic compliance and *screw* isotropic compliance. In the first case, the force vector is parallel to the displacement vector and, at the same time, the torque axis is parallel to the rotation axis. The second case refers to the condition of parallelism between the wrench and twist screw axes.

In this investigation, the isotropic compliance condition is analyzed in the Special Euclidean Group SE(2) by considering a 3RRR planar parallel manipulator in a generic posture. The proposed control scheme decouples the effects of the applied force and moment on the end-effector displacement and rotation, ensuring the condition of parallelism between force and displacement vectors. A numerical example is presented and multibody simulations are performed to verify the effectiveness of the control system.

2 ISOTROPIC COMPLIANCE IN SE(3)

With reference to Fig. 1, point P represents the interaction point between the end-effector and the external environment. The generic system of applied loads can be reduced to a force $\phi\hat{\mathbf{j}}$, whose line of action passes through P, and to a torque $\mu\hat{\mathbf{u}}$. The unit vector $\hat{\mathbf{k}}$, belonging to the plane defined by $\hat{\mathbf{j}}$ and $\hat{\mathbf{u}}$, is perpendicular to $\hat{\mathbf{j}}$ with the same sense of the component of $\hat{\mathbf{u}}$ perpendicular to $\hat{\mathbf{j}}$. From the definition of $\hat{\mathbf{j}}$ and $\hat{\mathbf{k}}$, it follows that $\hat{\mathbf{i}} = \hat{\mathbf{j}} \times \hat{\mathbf{k}}$. The reference frame $R_P \equiv \{P, x, y, z\}$ has origin in P and axes x, y, and z, defined by the unit vectors $\hat{\mathbf{i}}$, $\hat{\mathbf{j}}$, and $\hat{\mathbf{k}}$, respectively.

By resorting to the screw formulation, it is possible to introduce the wrench

$$\mathbf{w} = \begin{Bmatrix} \phi\hat{\mathbf{j}} \\ \mu\hat{\mathbf{u}} \end{Bmatrix} = \phi \begin{Bmatrix} \hat{\mathbf{j}} \\ \lambda\hat{\mathbf{j}} + \mathbf{p} \times \hat{\mathbf{j}} \end{Bmatrix}, \tag{1}$$

where λ is the wrench pitch and the vector $\mathbf{p} = p\hat{\mathbf{i}}$ defines the position of the point O belonging to the wrench axis O. The planes π and σ are normal to the unit vectors $\hat{\mathbf{k}}$ and $\hat{\mathbf{u}}$, respectively.

The wrench $\mathbf{w}$ is energetically conjugated [24] to the twist

$$\mathbf{t} = \begin{Bmatrix} \Delta\Theta\hat{\mathbf{h}} \\ \Delta\mathrm{P}\hat{\mathbf{v}} \end{Bmatrix} = \Delta\Theta \begin{Bmatrix} \hat{\mathbf{h}} \\ v\hat{\mathbf{h}} + \mathbf{r} \times \hat{\mathbf{h}} \end{Bmatrix}, \tag{2}$$

where v is the twist pitch and $\hat{\mathbf{h}}$,perpendicular to the plane χ, is the unit vector of the twist screw axis, H. The vector $\mathbf{r}$ defines the position of point H and represents the minimum distance between H and P. The vectors $\Delta\Theta\hat{\mathbf{h}}$ and $\Delta\mathrm{P}\hat{\mathbf{v}}$ represent the magnitudes of the end-effector displacement and rotation, respectively.

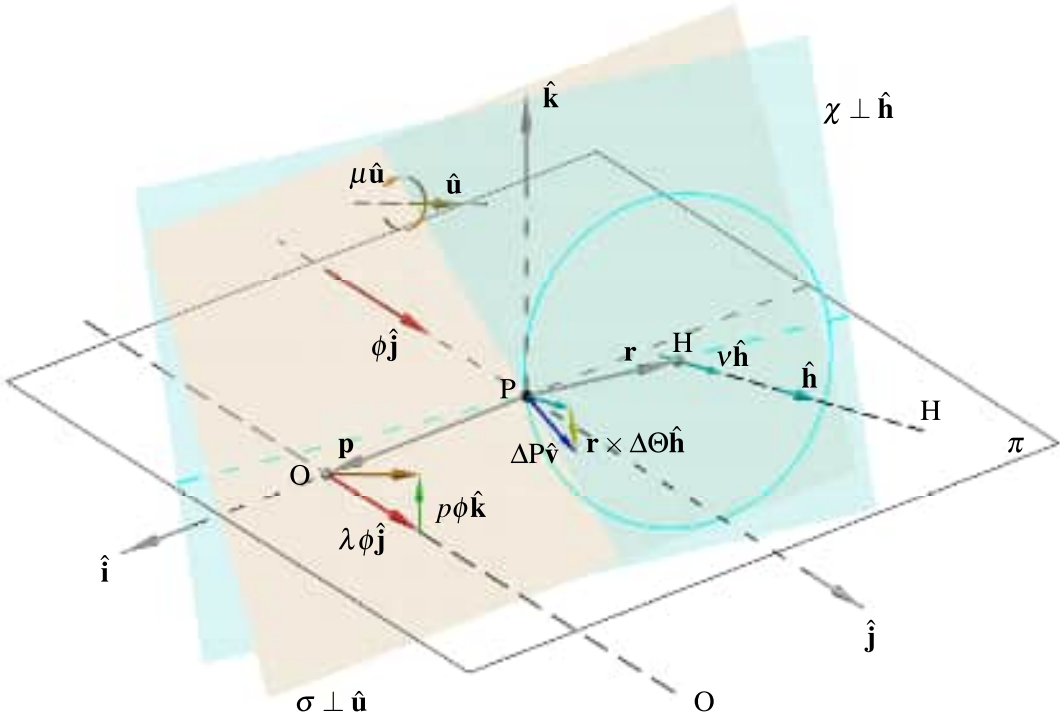

Figure 1. Wrench **w** and consequent twist **t** in the general case.

In general kinetostatic conditions, the manipulator posture and its dynamic characteristics determine the final pose of the end-effector. As a consequence, there are no specific relations between the unit vectors $\hat{\mathbf{j}}$ and $\hat{\mathbf{v}}$, that represent the directions of the applied force and the end-effector displacement, respectively. Analogously, there are no particular relations between the direction of the unit vectors $\hat{\mathbf{u}}$ and $\hat{\mathbf{h}}$, that represent the torque axis and the end-effector rotation axis, respectively.

The study presented in Ref. [21], focused on the Euclidean Group E(3), analyzed the relation between $\hat{\mathbf{j}}$ and $\hat{\mathbf{v}}$ and defined the condition of parallelism between the two unit vectors as *isotropic compliance* in E(3).

Subsequent studies [23, 22] considered the Special Euclidean Group SE(3) and, analyzing also the relations between the unit vectors $\hat{\mathbf{u}}$ and $\hat{\mathbf{h}}$, defined the following conditions.

- *Local* isotropic compliance: condition of parallelism between the unit vectors $\hat{\mathbf{j}}$ and $\hat{\mathbf{v}}$, and between the unit vectors $\hat{\mathbf{u}}$ and $\hat{\mathbf{h}}$. The displacement of the end-effector is parallel to the line of action of the applied force and its rotation axis is parallel to the axis of the applied torque.
- *Screw* isotropic compliance: condition of parallelism between the unit vectors $\hat{\mathbf{j}}$ and $\hat{\mathbf{h}}$. The screw axis of the twist is parallel to the screw axis of the applied wrench.

In the next Sections, the local isotropic compliance property is examined considering the planar parallel 3RRR manipulator.

3 LOCAL ISOTROPIC COMPLIANCE

According to the definition of local isotropic compliance in SE(3), the direction of the end-effector displacement must be parallel to the line of action of applied force, therefore

$$\hat{\mathbf{v}} = \hat{\mathbf{j}} \,. \tag{3}$$

Furthermore, the rotation axis of the end-effector must be to the axis of the applied torque:

$$\hat{\mathbf{h}} = \hat{\mathbf{u}} \,. \tag{4}$$

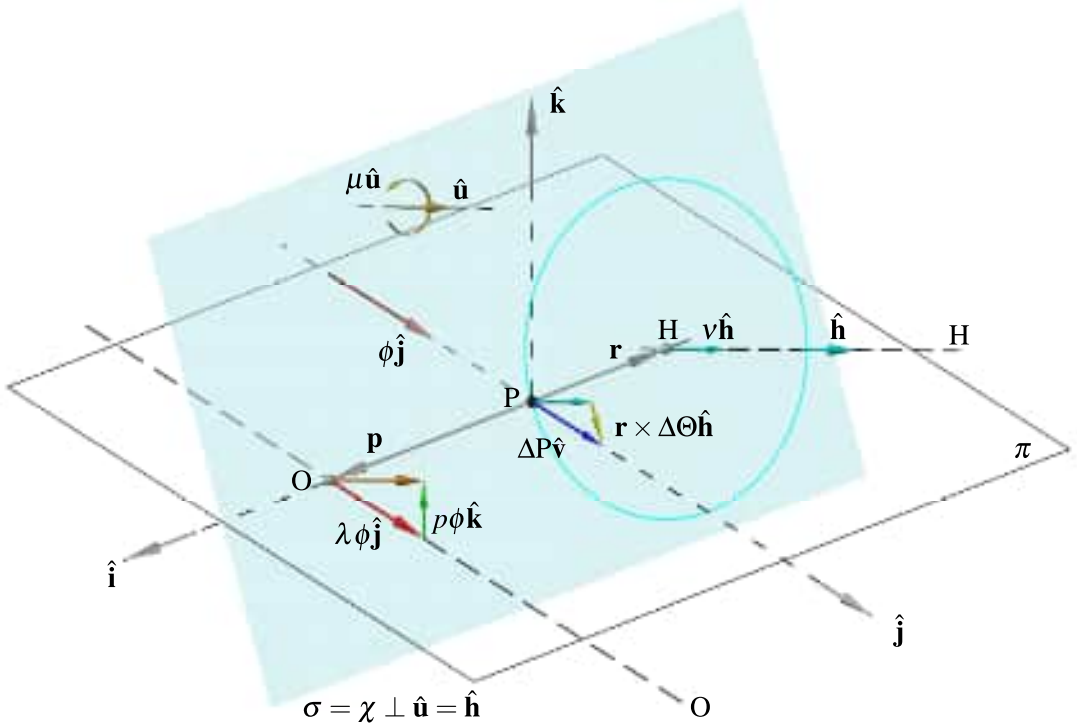

Figure 2. Local isotropic compliance. Wrench $\mathbf{w}$ and consequent twist $\mathbf{t}$, with $\hat{\mathbf{j}}=\hat{\mathbf{v}}$ and $\hat{\mathbf{u}}=\hat{\mathbf{h}}$.

From eqs. (1) and (2) it follows

$$\Delta P\hat{\mathbf{v}} \quad /\!/ \quad \phi\hat{\mathbf{j}}\,, \tag{5}$$
$$\Delta\Theta\hat{\mathbf{h}} \quad /\!/ \quad \mu\hat{\mathbf{u}}\,, \tag{6}$$

and

$$\Delta\Theta\left(v\hat{\mathbf{h}}+\mathbf{r}\times\hat{\mathbf{h}}\right) \quad /\!/ \quad \phi\hat{\mathbf{j}}\,, \tag{7}$$
$$\Delta\Theta\hat{\mathbf{h}} \quad /\!/ \quad \phi\left(\lambda\hat{\mathbf{j}}+\vec{p}\times\hat{\mathbf{j}}\right)\,. \tag{8}$$

The local isotropic compliance condition is illustrated in Fig. 2. The conditions of parallelism in section 3 and section 3 can be formulates as

$$\Delta P\hat{\mathbf{v}} = c_d\phi\hat{\mathbf{j}} \tag{9}$$

and

$$\Delta\Theta\hat{\mathbf{h}} = c_r\mu\hat{\mathbf{u}}\,, \tag{10}$$

respectively, where c_d and c_r are scalars. In matrix form, eqs. (9) and (10) can be rearranged as

$$\Delta\mathbf{S} = \mathbf{C}\mathbf{w}\,, \tag{11}$$

with

$$\mathbf{C} = \begin{bmatrix} c_d\mathbf{I} & 0 \\ 0 & c_r\mathbf{I} \end{bmatrix} \tag{12}$$

and

$$\Delta\mathbf{S} = \mathbf{I}^{\mathrm{a}}\mathbf{t}\,, \tag{13}$$

where $\mathbf{I}$ and $\mathbf{I}^{\mathrm{a}}$ are the 3×3 identity and anti-diagonal identity matrices, respectively.

Equation 11 expresses a relationship between displacements and forces, and between rotations and torques. From a physical point of view, $\mathbf{C}$ is a compliance matrix and the scalars c_d and c_r take the role of translational and rotational compliance coefficients, with units of mN^{-1} and $(\mathrm{N}\cdot\mathrm{m})^{-1}$, respectively.

On the other hand, the compliance matrix of a robotic manipulator is defined in the task space as

$$\mathbf{C} = \mathbf{J}\mathbf{k}^{-1}\mathbf{J}^{\mathrm{T}}\,. \tag{14}$$

In the previous relation, $\mathbf{J}$ is the manipulator jacobian defined as

$$\Delta\mathbf{S} = \mathbf{J}\Delta\mathbf{q}\,, \tag{15}$$

where $\Delta\mathbf{q}$ represents the variation of the joint coordinates vector. The matrix $\mathbf{k}$ is the manipulator stiffness matrix, defined in the joint space. Since $\mathbf{J}$ is posture-dependent and $\mathbf{C}$ depends both on $\mathbf{J}$ and $\mathbf{k}$, the compliance matrix obtained by means of eq. (14) is generally different from the matrix defined in eq. (12).

However, the stiffness matrix $\mathbf{k}$ generally depends on the mechanical characteristics of the manipulator, represented by the passive stiffness matrix $\mathbf{k}_{\mathrm{p}}$, and on the action exerted by the control system, represented by the control matrix $\mathbf{k}_{\mathrm{c}}$. In case of active stiffness regulation acting in parallel to the passive stiffness of the joints, $\mathbf{k}$ can be calculated as [21]

$$\mathbf{k} = \mathbf{k}_{\mathrm{p}} + \mathbf{k}_{\mathrm{c}}\,. \tag{16}$$

Therefore, the control matrix $\mathbf{k}_{\mathrm{c}}$ can be exploited to transform the compliance matrix of the manipulator in the scalar-like matrix in eq. (12) that guarantees the achievement of the local isotropic compliance property.

4 CONTROL ACTION DETERMINATION

Local isotropic compliance can be achieved by considering a control strategy based on active stiffness regulation. Considering only the contribution of the passive stiffness, the compliance matrix in the task space, obtained by means of eq. (14), can be partitioned as

$$\mathbf{C}_{\mathrm{p}} = \begin{bmatrix} \mathbf{A} & \mathbf{D} \\ \mathbf{D}^{\mathrm{T}} & \mathbf{B} \end{bmatrix}. \tag{17}$$

The passive stiffness matrix in the task space, that is the inverse of $\mathbf{C}_{\mathrm{p}}$, can be calculated as

$$\mathbf{K}_{\mathrm{p}} = \begin{bmatrix} \mathbf{E} & \mathbf{G} \\ \mathbf{G}^{\mathrm{T}} & \mathbf{H} \end{bmatrix}, \tag{18}$$

where

$$\mathbf{E} = \left(\mathbf{A} - \mathbf{D}\mathbf{B}^{-1}\mathbf{D}^{\mathrm{T}}\right)^{-1}, \tag{19}$$

$$\mathbf{G} = -\left(\mathbf{A} - \mathbf{D}\mathbf{B}^{-1}\mathbf{D}^{\mathrm{T}}\right)^{-1}\mathbf{D}\mathbf{B}^{-1}, \tag{20}$$

$$\mathbf{H} = \left(\mathbf{B} - \mathbf{D}^{\mathrm{T}}\mathbf{A}^{-1}\mathbf{D}\right)^{-1}. \tag{21}$$

By resorting to the spectral decomposition, the passive stiffness matrix can be written as

$$\mathbf{K}_{\mathrm{p}} = \begin{bmatrix} \mathbf{U}_{\mathrm{E}}\mathbf{\Sigma}_{\mathrm{E}}\mathbf{U}_{\mathrm{E}}{}^{\mathrm{T}} & \mathbf{G} \\ \mathbf{G}^{\mathrm{T}} & \mathbf{U}_{\mathrm{H}}\mathbf{\Sigma}_{\mathrm{H}}\mathbf{U}_{\mathrm{H}}{}^{\mathrm{T}} \end{bmatrix}, \tag{22}$$

where the columns of $\mathbf{U}_{\mathrm{E}}$, $\mathbf{U}_{\mathrm{H}}$ form a set of orthonormal eigenvectors of $\mathbf{E}$ and $\mathbf{H}$, respectively, and $\mathbf{\Sigma}_{\mathrm{E}}$, $\mathbf{\Sigma}_{\mathrm{H}}$ are diagonal matrices with the eigenvalues of $\mathbf{E}$ and $\mathbf{H}$, respectively.

To achieve local isotropic compliance, the control system must exert a generalized force in the task space that must satisfy two requirements. The first one is decoupling the the effects of the applied force and torque on the end-effector displacement and rotation. The second one is obtaining the parallelism condition between force and displacement and between torque axis and rotation axis. By focusing on the stiffness matrix, the first requirement is satisfied by zeroing out the elements of the off-diagonal blocks, whereas the second requirement is satisfied by transforming the diagonal blocks in scalar submatrices. By setting the generalized control force as

$$\begin{Bmatrix} \mathbf{f}_\mathrm{c} \\ \mathbf{m}_\mathrm{c} \end{Bmatrix} = \begin{bmatrix} \Delta\mathbf{E} & -\mathbf{G} \\ -\mathbf{G}^\mathrm{T} & \Delta\mathbf{H} \end{bmatrix} \begin{Bmatrix} \Delta\mathrm{P}\hat{\mathbf{v}} \\ \Delta\Theta\hat{\mathbf{h}} \end{Bmatrix}, \tag{23}$$

with

$$\Delta\mathbf{E} = \mathbf{U}_\mathrm{E}\left(\frac{1}{c_d}\mathbf{I} - \mathbf{\Sigma}_\mathrm{E}\right)\mathbf{U}_\mathrm{E}{}^\mathrm{T}, \qquad \Delta\mathbf{H} = \mathbf{U}_\mathrm{H}\left(\frac{1}{c_r}\mathbf{I} - \mathbf{\Sigma}_\mathrm{H}\right)\mathbf{U}_\mathrm{H}{}^\mathrm{T},$$

where c_d and c_r are the desired translational and rotational compliance coefficients. Therefore, by considering eq. (22) and

$$\mathbf{K}_\mathrm{c} = \begin{bmatrix} \Delta\mathbf{E} & -\mathbf{G} \\ -\mathbf{G}^\mathrm{T} & \Delta\mathbf{H} \end{bmatrix}, \tag{24}$$

the overall stiffness matrix in the task space becomes

$$\mathbf{K} = \mathbf{K}_\mathrm{p} + \mathbf{K}_\mathrm{c} = \begin{bmatrix} \frac{1}{c_d}\mathbf{I} & \mathbf{0} \\ \mathbf{0} & \frac{1}{c_r}\mathbf{I} \end{bmatrix}. \tag{25}$$

By calculating the inverse matrix of $\mathbf{K}$, the overall compliance matrix defined in eq. (12) is obtained, and the manipulator satisfies the local isotropic compliance condition in the considered posture. It is worth noting that the control stiffness matrix in eq. (24), defined in the task space, can be mapped into the joint space as

$$\mathbf{k}_\mathrm{c} = \mathbf{J}^\mathrm{T}\mathbf{K}_\mathrm{c}\mathbf{J}. \tag{26}$$

5 EXAMPLE IN SE(2): THE 3RRR PARALLEL MANIPULATOR

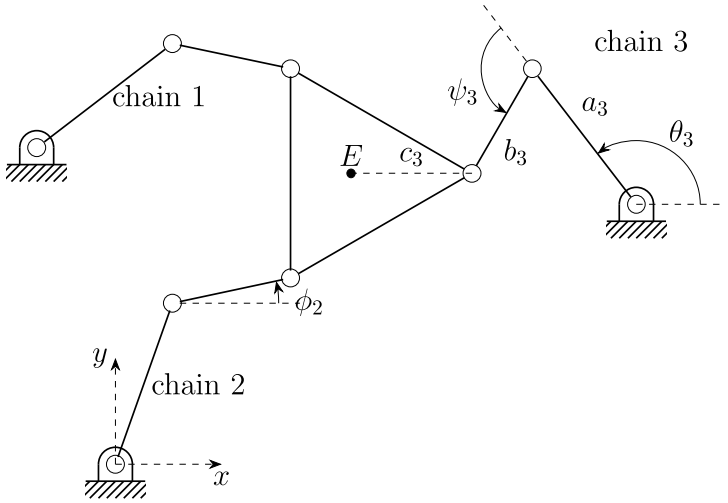

Figure 3. 3RRR robot: nomenclature.

With reference to Fig. 3, the posture of the planar manipulator is defined by the joint coordinates vector $\mathbf{q} = [\theta_1, \theta_2, \theta_3]^T$, whereas the end-effector pose in the task space is defined by $\mathbf{x} = [x_E, y_E, \phi]^T$. The regulation is exerted by the active joints connecting the manipulator to the

frame. Each actuated joint embed also the stiffness of the system, therefore the passive stiffness matrix of the manipulator is diagonal and defined as

$$\mathbf{k}_{\mathrm{p}} = \mathrm{diag}\{k_{p_1}, k_{p_2}, k_{p_3}\}\,. \tag{27}$$

The relation between the variation of the task and joint coordinates can be expressed as

$$\Delta\mathbf{x} = \mathbf{J}\Delta\mathbf{q}\,, \tag{28}$$

where

$$\mathbf{J} = \mathbf{J}_{\mathrm{x}}^{-1}\mathbf{J}_{\mathrm{q}} = \begin{bmatrix} b_{1x} & b_{1y} & c_{1x}b_{1y} - c_{1y}b_{1x} \\ b_{2x} & b_{2y} & c_{2x}b_{2y} - c_{2y}b_{2x} \\ b_{3x} & b_{3y} & c_{3x}b_{3y} - c_{3y}b_{3x} \end{bmatrix} \begin{bmatrix} a_{1x}b_{1y} - a_{1y}b_{1x} & 0 & 0 \\ 0 & a_{2x}b_{2y} - a_{2y}b_{2x} & 0 \\ 0 & 0 & a_{3x}b_{3y} - a_{3y}b_{3x} \end{bmatrix} \tag{29}$$

is the robot jacobian matrix. The values of the joint coordinates in the assigned posture $\mathbf{q}_{\mathrm{e}}$, that must not correspond to a kinematic singularity, are reported in Table 1. The table lists also the stiffness coefficients and link lengths of the manipulator under study.

Table 1. Values of the kinetostatic parameters of the manipulator.

	θ_i (rad)	k_{p_i} (N·m)	a_i (m)	b_i (m)	c_i (m)
1	0.65	800	$\sqrt{2}$	1	1
2	1.23	880	$\sqrt{2}$	1	1
3	2.23	710	$\sqrt{2}$	1	1

To achieve the isotropic compliance condition in $\mathbf{q}_{\mathrm{e}}$, the first step is to assign the desired compliance coefficients,

$$c_d = 2.\mathrm{E}-3\ \mathrm{m}\cdot\mathrm{N}^{-1}\,, \qquad c_r = 2.\mathrm{E}-3\ (\mathrm{N}\cdot\mathrm{m})^{-1}\,.$$

The second step consists of evaluating the jacobian matrix, that is

$$\mathbf{J}(q_{\mathrm{e}}) = \begin{bmatrix} -0.9096 & 0.1933 & 0.6911 \\ -0.8112 & -0.1724 & -0.616 \\ -0.3827 & -0.6628 & -0.6628 \end{bmatrix}, \tag{30}$$

and the compliance matrix in the task space. By substituting eqs. (27) and (30) in eq. (14), it follows

$$\mathbf{C}_{\mathrm{p}} = \begin{bmatrix} 8.094\mathrm{E}-4 & -7.476\mathrm{E}-4 & 2.802\mathrm{E}-4 \\ -7.476\mathrm{E}-4 & 9.562\mathrm{E}-3 & -4.679\mathrm{E}-3 \\ 2.802\mathrm{E}-4 & -4.679\mathrm{E}-3 & 3.272\mathrm{E}-3 \end{bmatrix}. \tag{31}$$

The third step consists of calculating, according to eq. (18), the stiffness matrix K_{p} in the task space. Then, the submatrices **E**, **G**, and **H** can be determined by means of eq. (19), eq. (20), and eq. (21), respectively. Finally, the control stiffness matrices are evaluated. In the task space, from eq. (24) it follows

$$\mathbf{K}_{\mathrm{c}} = \begin{bmatrix} -844.92 & -162.49 & -117.18 \\ -162.49 & 132.00 & -512.33 \\ -117.18 & -512.33 & -528.22 \end{bmatrix}, \tag{32}$$

whereas in the joint space, considering eq. (26), it follows

$$\mathbf{k}_{\mathrm{c}} = \begin{bmatrix} -101.55 & -844.81 & 848.89 \\ -844.81 & 1422.74 & -2067.89 \\ 848.89 & -2067.89 & 1655.70 \end{bmatrix}. \tag{33}$$

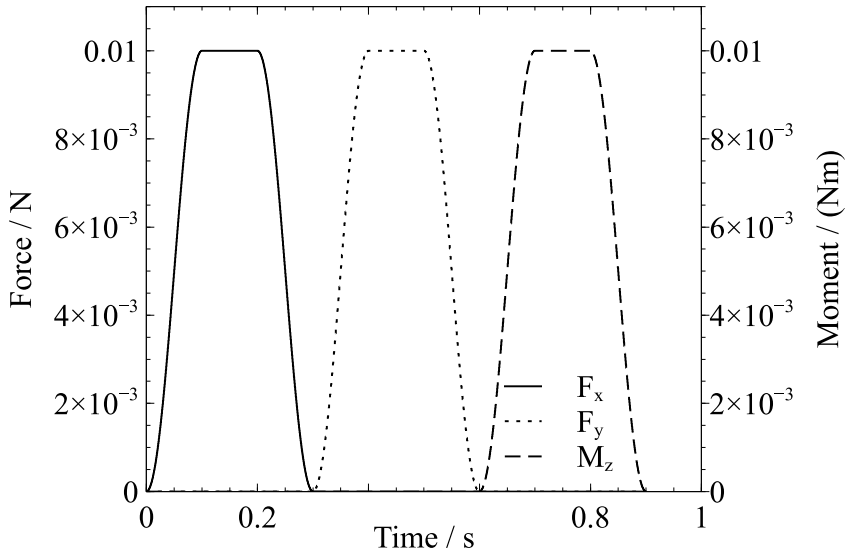

Figure 4. End effector disturbance force and moment.

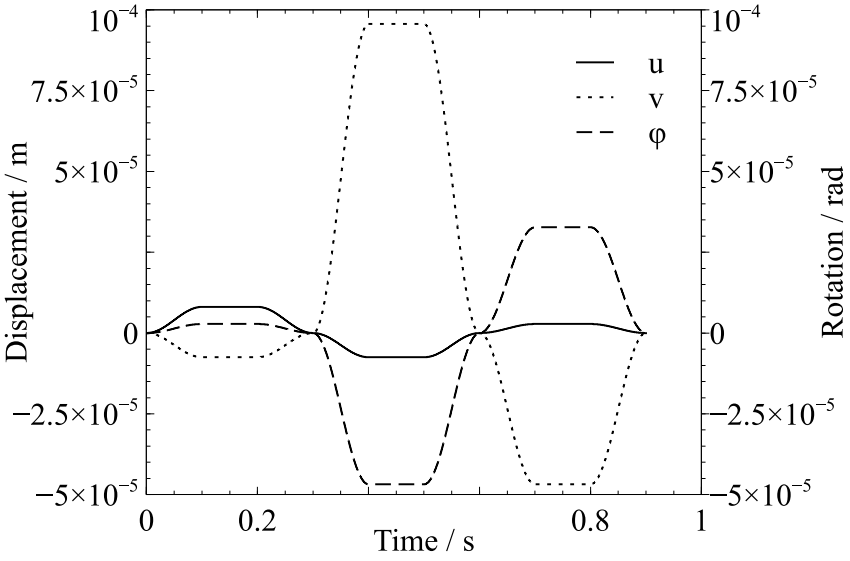

Figure 5. End effector displacement and rotation, system with no control.

6 MULTIBODY SIMULATION

The response of the system was simulated using MBDyn[1], a free general-purpose multibody solver developed at Politecnico di Milano [25, 26, 27]. The manipulator model, whose kinematic is constrained on the $x-y$ plane, consists of seven rigid bodies and nine revolute joints. Each joint has a nominal torsional stiffness k_p (Table 1); an additional very small damping term, equal to $2 \cdot 10^{-4} \cdot k_p$ N$\cdot$m$\cdot$s$\cdot$rad^{-1}, is added in order to stabilize the analysis. The inertia properties of the links are not relevant in this context since the loads have been applied in quasi-static condition.

A sequence of two independent disturbance forces and a moment, shown in Fig. 4, is applied to the end-effector. The two forces are directed along the coordinate axes of the plane, whereas the moment is about an axis perpendicular to the plane. The magnitude of each force is 0.2 N, whereas the moment magnitude is 0.2 N·m. These values have been chosen so that the corresponding configuration change is small enough to make kinematic nonlinearities in the perturbed solution negligible. Each force and moment is slowly increased following a regular $(1-\cos(t))$ pattern, then kept constant, and subsequently brought back to zero following the reverse pattern

[1] `http://www.mbdyn.org/`, last accessed March 2023.

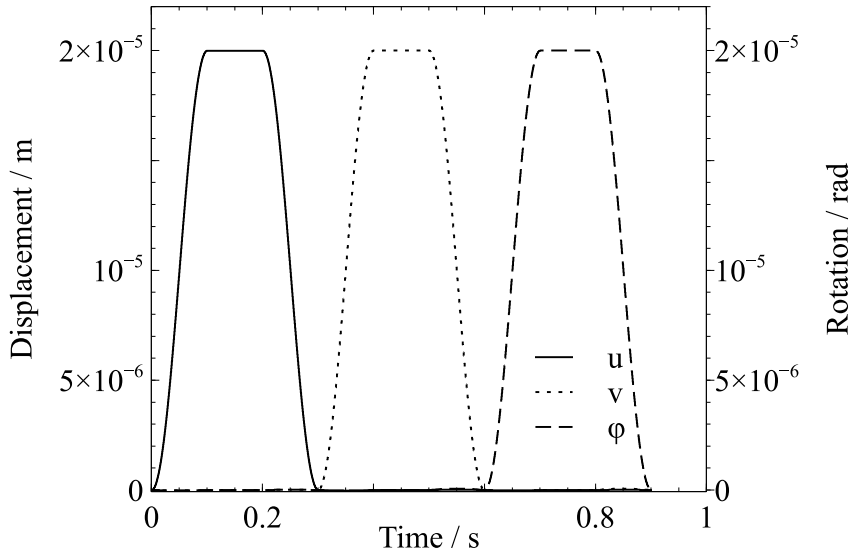

Figure 6. End effector displacement and rotation, controlled system.

$(\cos(t) - 1)$. The small applied loads induce correspondingly small configuration changes; thus, the feedback gain matrix, eq. (26), can be kept constant.

The results presented in Figs. 5 and 6 show the two components of displacement, u and v, and the finite rotation, φ, of the end effector, respectively computed with and without the control action. They clearly show how the system response is coupled without feedback action, while the feedback allow to achieve an almost ideal isotropic compliance. This is the case both for when the end-effector is loaded with a force and when it is loaded with a moment; both type of loading lead to the qualitatively identical responses.

7 CONCLUSIONS

In this paper, the local isotropic compliance property has been studied in SE(2) by considering a planar parallel 3RRR manipulator in a generic posture. A proper control strategy has been developed to decouple the effects of the external actions on the end-effector displacement and rotation. The manipulator behavior has been simulated by means of the MB-Dyn software, by considering different load cases. For each case, the results show the effectiveness of the control action in determining an isotropic compliant response.

REFERENCES

[1] Kim, H.W., Lee, J.H., Suh, I.H., Yi, B.J.: Comparative study and experimental verification of singular-free algorithms for a 6 DOF parallel haptic device. Mechatronics **15**(4) (may 2005) 403–422

[2] Gallardo-Alvarado, J., Alici, G., Pérez-González, L.: A new family of constrained redundant parallel manipulators. Multibody System Dynamics **23**(1) (sep 2009) 57–75

[3] Zhao, Y., Gao, F.: Dynamic performance comparison of the 8pss redundant parallel manipulator and its non-redundant counterpart—the 6pss parallel manipulator. Mechanism and Machine Theory **44**(5) (may 2009) 991–1008

[4] Patel, Y.D., George, P.M.: Parallel manipulators applications—a survey. Modern Mechanical Engineering **02**(03) (2012) 57–64

[5] Li, H., min Zhang, X., Zeng, L., jiang Huang, Y.: A monocular vision system for online pose measurement of a 3rrr planar parallel manipulator. Journal of Intelligent and Robotic Systems **92**(1) (oct 2017) 3–17

[6] Si, G., Chen, F., Zhang, X.: Comparison of the dynamic performance of planar 3-DOF parallel manipulators. Machines **10**(4) (mar 2022) 233

[7] Wu, J., Wang, J., Wang, L., You, Z.: Performance comparison of three planar 3-DOF parallel manipulators with 4-RRR, 3-RRR and 2-RRR structures. Mechatronics **20**(4) (jun 2010) 510–517

[8] Saheb, S., Babu, G.: Mathematical modeling and kinematic analysis of 3-RRR planar parallel manipulator. EAI Endorsed Transactions on Energy Web (jul 2018) 168502

[9] Arsenault, M., Boudreau, R.: The synthesis of three-degree-of-freedom planar parallel mechanisms with revolute joints (3-RRR) for an optimal singularity-free workspace. Journal of Robotic Systems **21**(5) (2004) 259–274

[10] Chang, F.: Kinematical performance analysis for planar parallel mechanism 3rrr. Chinese Journal of Mechanical Engineering (English Edition) **17**(supp) (2004) 181

[11] Bonev, I.A., Zlatanov, D., Gosselin, C.M.: Singularity analysis of 3-DOF planar parallel mechanisms via screw theory. Journal of Mechanical Design **125**(3) (sep 2003) 573–581

[12] Liu, S., cheng Qiu, Z., min Zhang, X.: Singularity and path-planning with the working mode conversion of a 3-DOF 3-RRR planar parallel manipulator. Mechanism and Machine Theory **107** (jan 2017) 166–182

[13] Zhan, Z., Zhang, X., Zhang, H., Chen, G.: Unified motion reliability analysis and comparison study of planar parallel manipulators with interval joint clearance variables. Mechanism and Machine Theory **138** (aug 2019) 58–75

[14] Ghorbel, F., Chetelat, O., Gunawardana, R., Longchamp, R.: Modeling and set point control of closed-chain mechanisms: theory and experiment. IEEE Transactions on Control Systems Technology **8**(5) (2000) 801–815

[15] Su, Y., Sun, D., Ren, L., Wang, X., Mills, J.: Nonlinear PD synchronized control for parallel manipulators. In: Proceedings of the 2005 IEEE International Conference on Robotics and Automation, IEEE

[16] Codourey, A.: Dynamic modeling of parallel robots for computed-torque control implementation. The International Journal of Robotics Research **17**(12) (dec 1998) 1325–1336

[17] Honegger, M., Codourey, A., Burdet, E.: Adaptive control of the hexaglide, a 6 dof parallel manipulator. In: Proceedings of International Conference on Robotics and Automation, IEEE

[18] Zubizarreta, A., Marcos, M., Cabanes, I., Pinto, C., Portillo, E.: Redundant sensor based control of the 3rrr parallel robot. Mechanism and Machine Theory **54** (aug 2012) 1–17

[19] Huynh, B.P., Kuo, Y.L.: Dynamic filtered path tracking control for a 3rrr robot using optimal recursive path planning and vision-based pose estimation. IEEE Access **8** (2020) 174736–174750

[20] Kuo, Y.L., Tang, S.C.: Dynamics and control of a 3-DOF planar parallel manipulator using visual servoing resolved acceleration control. Journal of Low Frequency Noise, Vibration and Active Control **40**(1) (oct 2019) 458–480

[21] Belfiore, N.P., Verotti, M., Di Giamberardino, P., Rudas, I.J.: Active joint stiffness regulation to achieve isotropic compliance in the euclidean space. Journal of Mechanisms and Robotics **4**(4) (2012) 041010 1–11

[22] Verotti, M., Masarati, P., Morandini, M., Belfiore, N.: Isotropic compliance in the special euclidean group SE(3). Mechanism and Machine Theory **98** (apr 2016) 263–281

[23] Verotti, M., Masarati, P., Morandini, M., Belfiore, N.P.: Active isotropic compliance in redundant manipulators. Multibody System Dynamics **49**(4) (jan 2020) 421–445

[24] Merlini, T., Morandini, M.: The helicoidal modeling in computational finite elasticity. part i: Variational formulation. International Journal of Solids and Structures **41**(18-19) (2004) 5351–5381

[25] Masarati, P., Morandini, M., Quaranta, G., Mantegazza, P.: Open-source multibody software. In: Proceedings of Multibody Dynamics 2003 International Conference on Advances in Computational Multibody Dynamics, Lisboa, Portugal (July 1-4 2003)

[26] Masarati, P., Morandini, M., Mantegazza, P.: An efficient formulation for general-purpose multibody/multiphysics analysis. Journal of Computational and Nonlinear Dynamics **9**(4) (July 2014) 041001–041001

[27] Zhang, H., Zhang, R., Zanoni, A., Masarati, P.: Performance of implicit a-stable time integration methods for multibody system dynamics. Multibody System Dynamics **54**(3) (jan 2022) 263–301